Tellus (1982), *34*, 514–525

A seasonal global climate model with an equivalent meridional atmospheric circulation

By E. ELIASEN and L. LAURSEN, *Institute of Theoretical Meteorology, University of Copenhagen, Haraldsgade 6, DK-2200 Copenhagen N, Denmark*

(Manuscript received November 26, 1981; in final form February 22, 1982)

ABSTRACT

A seasonal, zonally averaged, climate model is developed using a hypothetical meridional circulation, which reproduces the atmospheric dynamical heating of a two-level general circulation model. In order to simulate the seasonal temperature cycle, prognostic equations for the land and ocean temperatures are included in the model. The horizontal heat transport in the ocean is modelled as ordinary diffusion. Small-scale vertical transport of sensible and latent heat is described by simple linear terms. For the long-wave radiation calculations, a simple but efficient emissivity approximation scheme is developed. The short-wave radiation treatment is based on an early version of the Mintz-Arakawa general circulation model.

The meridional and seasonal variation of the surface temperature as well as the temperature at the two tropospheric levels are simulated quite well by the model. Concerning surface albedo and planetary albedo, the model gives results which are in good agreement with observed values. Radiative fluxes of the model also compare well with observed values.

The sensitivity of the model to changes in incoming solar radiation and carbon dioxide content is in accordance with results obtained from other models. The model, with variation of the Earth's orbital parameters, has also been used for some preliminary experiments.

1. Introduction

Essentially the climate modelling problem may be divided into two parts. The first one is concerned with the basic physical processes like short- and long-wave radiation, vertical small-scale transport of heat and water vapour, condensation, evaporation, freezing and melting, all processes which numerically may be described inside a vertical column of the atmosphere–earth system. The other fundamental part of the climate modelling problem is concerned with the very important redistribution of heat and humidity by the large-scale motions of the atmosphere and the oceans. A detailed numerical description in space and time of these motions involves an enormous amount of computational work, which has advanced the idea, that for modelling of long-term climate changes, the effect of the large-scale motions should be incorporated in a parameterized form.

In a recent paper (Eliasen, 1982) it was proposed that a usable parameterization of the large-scale atmospheric heat transport in a zonally averaged climate model could be obtained by defining a hypothetical equivalent meridional circulation, equivalent in the sense that this meridional circulation should produce the same dynamical heating as the mean heating caused by the total large-scale motions. The crucial point of such a parameterization is of course to define the hypothetical meridional circulation in terms of the zonally averaged temperature field. This was attempted on the basis of the long-term statistics obtained from a simplified two-layer general circulation model, and it was found, that an equivalent meridional circulation in the analogous climate model could be determined in a quite elementary way.

In the present paper, the proposed parameterization of the large-scale atmospheric heat transport is tested by applying it to a climate

0040-2826/82/060514-12$02.50/0

model, which may be considered as essentially an improved version of the original one. An important change is that the heating due to the radiation processes is treated in a more realistic—though still simple—way. Concerning the solar forcing of the model, the incoming radiation is computed as a function of latitude and time, whereby the basic features of seasonal variations are incorporated in the model. Another essential change is the use of explicit prognostic equations for the changes in the surface temperatures of land- and ocean-areas. Provisionally these equations are kept simple, but in principle they provide the possibility for the processes in the surface layers and the large-scale heat transport in the oceans to be taken into account in a more realistic way.

As a first goal it is shown that the model gives a reasonably good simulation of the observed meridional and seasonal variations of the zonally averaged temperature. Furthermore the model has been applied to some conventional sensitivity experiments with quite reasonable results.

2. Model description

The temperature of the troposphere is represented by the zonally averaged temperature fields T_1 and T_3 at the pressure levels $p_1 = 400$ mb and $p_3 = 800$ mb, respectively. These two temperature fields as functions of time t and latitude ϕ are to be determined from the thermodynamic equation applied in the zonally averaged form at the two levels p_1 and p_3. Using the parameterization of the total large-scale heat transport in terms of an equivalent meridional circulation as proposed by Eliasen (1982), the two equations for T_1 and T_3 become

$$\frac{\partial T_1}{\partial t} + E\left\{r_1\sigma(\theta_2 - [\theta_2]) - q_1\frac{\partial\beta}{\partial\phi}\frac{\partial T_1}{\partial\phi}\right\} = \frac{Q_1}{c_p},$$

$$\frac{\partial T_3}{\partial t} + E\left\{r_3\sigma(\theta_2 - [\theta_2]) + q_3\frac{\partial\beta}{\partial\phi}\frac{\partial T_3}{\partial\phi}\right\} = \frac{Q_3}{c_p}, \tag{2.1}$$

where $\theta_2 = \frac{1}{2}(\theta_1 + \theta_3)$ and $\sigma = \frac{1}{2}(\theta_1 - \theta_3)$. θ denotes the potential temperature and

$$T = r\theta, \qquad r = \left(\frac{p}{p_*}\right)^\kappa,$$

where $p_* = 1000$ mb and $\kappa = R/c_p$ with R being the gas constant and c_p the specific heat capacity of air at constant pressure. The symbol [ ] indicates the horizontal mean value over the whole sphere. The field β may be considered as a smoothed temperature field, defined by the relation

$$\frac{\partial\left(\cos\phi\dfrac{\partial\beta}{\partial\phi}\right)}{\cos\phi\,\partial\phi} = [\theta_2] - \theta_2, \qquad [\beta] = 0. \tag{2.2}$$

The coefficient E is introduced as determining the intensity of the equivalent meridional circulation. Its possible dependence upon the global parameters of the system was discussed in Eliasen (1982), where the "normal" value $E = 3.1 \cdot 10^{-8}$ K^{-1} s^{-1} was also stated, a value which is used throughout in the present application of the model. Furthermore the values of q_1 and q_3 were given as

$$q_1 = 1 + \frac{r_3 - r_1}{2r_1} = 1.1097,$$

$$q_3 = 1 - \frac{r_3 - r_1}{2r_3} = 0.9100,$$

where the deviations from the value 1 are due to a crude incorporation of the frictional heating in the dynamical heating. Thus, the quantities Q_1 and Q_3 on the right-hand-side of eqs. (2.1) represent the heating rates per unit mass for that part of the heating due to the radiation processes and to the small-scale vertical heat transport. In terms of the absorbed solar radiation A, the upward net fluxes of long-wave radiation F and small-scale heat transport H, the heating rates may be written

$$Q_1 = \frac{g}{\Delta p}(A_1 + F_M - F_T + H_M),$$

$$Q_3 = \frac{g}{\Delta p}(A_3 + F_S - F_M + H_S - H_M), \tag{2.3}$$

where g is the acceleration of gravity, $\Delta p = 400$ mb and where the indices T, M and S refer to the 200 mb level, the 600 mb level and the surface, respectively.

Certainly the surface temperature is of decisive importance for the energy exchange between the atmosphere and the surface, and a realistic climate model must therefore also include the surface temperature as a basic variable. Due to

the large difference in the effective heat capacity between land and ocean surfaces, it seems furthermore appropriate to distinguish between the land surface temperature T_L and the ocean surface temperature T_W in order to model the seasonal cycle (*cf.* Thompson and Schneider, 1979). The zonally averaged surface temperature T_S may then be written

$$T_S = fT_W + (1-f)T_L, \tag{2.4}$$

where f is the fraction of the latitude circle covered by ocean. Analogous expressions are used for F_S and H_S.

The prognostic equation of the land surface temperature is

$$C_L \frac{\partial T_L}{\partial t} = A_L - F_L - H_L, \tag{2.5}$$

where C_L is the heat capacity of the land surface, A_L the solar radiation absorbed by the surface, F_L the net upward long-wave radiation and H_L the flux of sensible and latent heat from the surface to the atmosphere. The magnitude of the heat capacity C_L varies strongly with the physical properties of the surface, but in all cases the value of C_L is more than one order of magnitude smaller than the heat capacity C_W of the upper mixed layer of the ocean. In the numerical experiments with the present model, C_L has been treated as a constant with a value of 50 W m^{-2} day K^{-1}.

Using the same symbols as in eq. (2.5) but with the index W, instead of L, indicating the ocean surface, the prognostic equation for the temperature T_W is written

$$C_W \frac{\partial T_W}{\partial t} = A_W - F_W - H_W + \frac{1}{f}\frac{\partial\left(K C_W \cos\phi \dfrac{\partial T_W}{\partial \phi}\right)}{\cos\phi\, \partial\phi}, \tag{2.6}$$

where the last term describes the horizontal heat diffusion. This treatment of the horizontal heat transport in the oceans is certainly a very crude one, but at least the chosen form generates a reasonable transport of heat from the equatorial area towards the poles. The intensity of the heat transport is determined by the coefficient K. Essentially the same expression for the large-scale heat transport in the oceans was used by Sellers (1973), with K varying with latitude. In the present model K is treated as a constant with the value $1.1 \cdot 10^{-4}$ day^{-1}, which is very close to the average value used by Sellers.

Quite recently Ghil and Bhattacharya (1979) have presented values of the heat capacity of the climate system due to the upper mixed layer of the ocean, and on the basis of these values the following expression for the heat capacity of the ocean areas has been adopted

$$C_W = C_0 - (C_0 - C_A)\, g(\mu), \tag{2.7}$$

where $\mu = \sin\phi$ and

$$g(\mu) = \begin{cases} 0, & |\mu| \leqslant \mu_A, \\ \left(\dfrac{|\mu| - \mu_A}{1 - \mu_A}\right)^2, & |\mu| \geqslant \mu_A. \end{cases}$$

The constant value C_0 is assumed to be 3000 W m^{-2} day K^{-1}, the value C_A is taken to be 100 W m^{-2} day K^{-1} and $\mu_A = 0.766$.

The heat balance between the atmosphere and the earth is critically influenced by the small-scale vertical transport of sensible heat and water vapour. Unfortunately only very little is known about an adequate parameterization of this transport in climate modelling, so a quite simple linear formulation is used in the present model. The upward flux from the ground to the atmosphere is written as two contributions

$$H_G = H_G^C + H_G^E, \tag{2.8}$$

representing the sensible heat and the latent heat, respectively. The index G indicates either land (L) or ocean (W) surfaces. For the sensible heat it is assumed that

$$H_G^C = \begin{cases} a_G(T_G - T_3 - \gamma_G), & T_G - T_3 \geqslant \gamma_G - 1, \\ -a_G, & T_G - T_3 \leqslant \gamma_G - 1, \end{cases} \tag{2.9}$$

which express a simple adjustment of the temperature difference $T_G - T_3$ towards the prescribed value γ_G. Using the reasonable value $\gamma_G = 6$ K, the expression (2.9) gives a heat transport from the ground to the atmosphere increasing with increasing values of $T_G - T_3$. If $T_G - T_3 < 6$ K,

corresponding to a strong vertical stability, the expression (2.9) yields a modest downward heat transport from the atmosphere to the surface with a maximum value equal to a_G.

An essential part of the vertical heat transport is connected with the evaporation from the earth's surface and the subsequent transport and condensation of water vapour in the atmosphere. As the content of water vapour is not explicitly determined in the present form of the model, the content must be parameterized using the temperature field. In a highly simplified way this is done by assuming that the relative humidity close to the ground has a prescribed constant value from which the mixing ratio q_G at the surface temperature T_G may be calculated. For the present integrations of the model it is assumed that the relative humidity has the same value for land and ocean surfaces, namely 80%. With the value of q_G obtained in this way the vertical heat transport connected with the water vapour is put proportional to q_G, i.e.

$$H_G^E = b_G q_G. \tag{2.10}$$

From the known mean values for the energy balance of the atmosphere–earth system, the following numerical values have been adopted: $a_G = 15$ W m^{-2} K^{-1} and $b_G = 4000$ W m^{-2}.

The energy transfer from the earth's surface to the atmosphere is linked to a further vertical transport from the lower to the upper layer as expressed in the model by the quantity H_M. In accordance with the simple expressions (2.8)–(2.10), H_M is written as

$$H_M = H_M^C + H_M^E, \tag{2.11}$$

with

$$H_M^C = \begin{cases} a_M(T_3 - T_1 - \gamma_M), & T_3 - T_1 \geqslant \gamma_M, \\ 0, & T_3 - T_1 \leqslant \gamma_M, \end{cases} \tag{2.12}$$

$$H_M^E = b_M\{f q_W + (1-f) q_L\}. \tag{2.13}$$

In the numerical experiments to be described, the following values have been used

$$a_M = 6 \text{ W m}^{-2} \text{ K}^{-1}, \qquad \gamma_M = 24 \text{ K},$$

$$b_M = 1000 \text{ W m}^{-2},$$

leading to reasonable values of the vertical heat transport.

3. Radiation calculations

3.1. *Solar radiation*

The incident solar flux S at the top of the atmosphere as a function of latitude and calendar date is computed from the astronomical parameters as mean values for each day during the year by the procedure outlined by Berger (1978). The origin of time is defined to be the vernal equinox, and the year to be 365 days.

In a cloudless atmosphere, the factors that cause depletion of solar radiation are absorption and scattering. Absorption and scattering by aerosols are neglected. Almost all atmospheric ozone, which has absorption bands for wavelengths less than 0.7 μm, is present above the 200 mb level. Absorption by ozone is accounted for by simply reducing the solar flux by about 4% from the top of the atmosphere to the 200 mb level. This is in agreement with explicit calculations based on the expressions for ozone absorption given by Lacis and Hansen (1974) using average values for total ozone amounts and zenith angles. The absorption bands of water vapour for wavelengths less than 0.9 μm are negligible, whereas Rayleigh scattering on the other hand is quite small for wavelengths larger than this limit. Above the 200 mb level there is minor absorption by water vapour which is set to about 1%. From these considerations, the downward solar flux at the 200 mb level is separated into a part S_r subject only to scattering and a part S_a subject only to absorption.

$$S_r = 0.61S, \qquad S_a = 0.34S. \tag{3.1}$$

With the assumption that reflected radiation is not absorbed, the absorption of S_a in the upper layer is taken to be

$$A_1^0 = A\{(U_T - U_M)M\} S_a. \tag{3.2}$$

M is the magnification factor given by Rodgers (1967)

$$M = \frac{35}{(1224\cos^2 Z + 1)^{1/2}}, \tag{3.3}$$

where Z is the effective mean zenith angle of the sun determined in the same way as by Manabe and Strickler (1964). U is the effective vapour amount from the ground to the pressure level indicated by the index. The absorption function used is the one given by Manabe and Müller (1961):

$$A(U) = 0.271U^{0.303}, \tag{3.4}$$

with U determined by the pressure corrected expression

$$U_p = \int_p^{p_s} q(p) \frac{p}{p_s} \frac{\mathrm{d}p}{g}. \tag{3.5}$$

In order to calculate U_p, the vertical profile of the mixing ratio $q(p)$ has to be known. In consideration of the general crudeness of the model, this profile is assumed to be the same above the land- and ocean-areas, and given by

$$q(p) = q_S \left(\frac{p}{p_S}\right)^m, \tag{3.6}$$

where q_S is determined from T_S and with the limitation that $q(p)$ is not less than $2.5 \cdot 10^{-6}$. It is assumed that m is independent of latitude and equal to 3. Having obtained the values for A_1^0, the absorption in the lower layer may be expressed as

$$A_3^0 = A\{U_T M\} S_a - A_1^0. \tag{3.7}$$

The effect of clouds is treated in a quite simple way by introducing a single cloud layer extending from p_{CB} to p_{CT}. p_{CB} is the pressure at the mean height of the cloud bottom, which is assumed to be in the range from 800 mb to 600 mb and independent of latitude and time. p_{CT} is the pressure at the mean height of the cloud top, and the cloud is assumed to be situated symmetrically around the 600 mb level. The absorption by the cloud is accounted for by using an equivalent cloud water vapour amount U_{CL} which is taken to be

$$U_{CL} = \frac{15 q_S}{0.005 + q_S}. \tag{3.8}$$

Following Langlois and Kwok (1969), the radiation stream is divided into two parts, one of which is reflected at the cloud top and the other of which enters the cloud. The latter part becomes diffuse and the mean path length is taken to be 1.66 times larger than that of the vertical column. With the water vapour content assumed to vary linearly with pressure within the cloud we have

$$\begin{aligned} A_1^C &= \alpha_{CT} S_a A\{(U_T - U_{CT}) M\} + B, \\ A_3^C &= (1 - \alpha_{CT}) S_a \\ &\quad A\{(U_T - U_{CT}) M + 1.66(U_{CT} + U_{CL})\} - B, \end{aligned} \tag{3.9}$$

where

$$\begin{aligned} B &= (1 - \alpha_{CT}) S_a \\ &\quad A\{(U_T - U_{CT}) M + 1.66(\tfrac{1}{2}U_{CL} + U_{CT} - U_M)\}. \end{aligned}$$

α_{CT} is the albedo at the top of the cloud given by

$$\alpha_{CT} = 0.36 + 0.0082(Z - 45°). \tag{3.10}$$

The value 0.36 is the cloud albedo for a mean zenith angle of 45°. This value is somewhat larger than that used by Thompson (1979) to compensate for the neglect of Rayleigh scattering above the cloud. The absorption in the two layers, with the fraction of overcast sky called CL, are

$$\begin{aligned} A_1 &= \mathrm{CL}\, A_1^C + (1 - \mathrm{CL})\, A_1^0, \\ A_3 &= \mathrm{CL}\, A_3^C + (1 - \mathrm{CL})\, A_3^0. \end{aligned} \tag{3.11}$$

The amount of absorption at the ground is dependent on the kind and condition of the surface. In the following α_G denotes any surface albedo, and it is assumed that α_G is the same for direct and diffuse radiation. For clear skies in the spectral region with water vapour absorption, the absorption at the ground is

$$A_{G,a}^0 = (1 - \alpha_G)(S_a - A_1^0 - A_3^0). \tag{3.12}$$

In that part of the spectrum where Rayleigh scattering occurs, we have for clear skies

$$A_{G,r}^0 = S(0.61 - R_r)(1 - \alpha_G)/(1 - \alpha_G R_r^*), \tag{3.13}$$

which accounts for multiple reflection between the ground and the Rayleigh atmosphere. In accordance with Lacis and Hansen (1974), R_r is the atmospheric albedo due to Rayleigh scattering given by

$$R_r = \frac{0.28}{1 + 6.43 \cos Z}. \tag{3.14}$$

R_r^* is the Rayleigh albedo for radiation from below, and the value used for R_r^* is 0.0685. With multiple reflection between the ground and the cloud base, the absorption in the scattered part of the spectrum is

$$A_{G,r}^C = S_r(1 - \alpha_G)(1 - \alpha_{CT})/(1 - \alpha_G \alpha_{CB}), \tag{3.15}$$

where the albedo of the cloud base α_{CB} is taken to be 0.45. For that part of the spectrum which is subject to absorption in the atmosphere, the expression for absorption at the ground becomes

$$A_{G,a}^C = (1 - \alpha_G)\{(1 - \alpha_{CT}) S_a - A_3^C - B\}/(1 - \alpha_G \alpha_{CB}). \tag{3.16}$$

The total absorption at the ground is then

$$A_G = CL(A^C_{G,a} + A^C_{G,r}) + (1 - CL)(A^0_{G,a} + A^0_{G,r}). \quad (3.17)$$

The surface albedo is a very important factor in climate modelling, especially due to the ice-albedo feedback. The parameterization of the surface as well as the planetary albedo in terms of the mean temperature field and zenith angle has been discussed in several recent papers. Following mainly the results of Thompson (1979), the parameterization used in the present model is given by

$$\alpha_L = \begin{cases} 0.16, & T_L \geqslant 283 \text{ K}, \\ 0.16 + 0.015(283 - T_L), & T_L < 283 \text{ K}; \end{cases} \quad (3.18)$$

$$\alpha_W = \begin{cases} 0.07 + 4 \cdot 10^{-6}(Z - 45°)^3, & T_W \geqslant 273 \text{ K}, \\ 0.07 + 4 \cdot 10^{-6}(Z - 45°)^3 + 0.06(273 - T_W), & 263 \text{ K} < T_W < 273 \text{ K}, \\ 0.67 + 4 \cdot 10^{-6}(Z - 45°)^3, & T_W \leqslant 263 \text{ K}, \end{cases} \quad (3.19)$$

with the albedo values restricted to be less than 0.75, except in the Antarctic area, where a fixed value of 0.85 is used in order to account for the permanent high-level ice sheet.

3.2. *Long-wave radiation*

The computation of the heating due to long-wave radiation follows the method developed by Sasamori (1968), modified in order to include radiation by clouds. In the case of no clouds the downward flux is given by

$$F^{0\downarrow}(p) = \sigma_B T_0^4 \varepsilon(p, 0) + \sigma_B \int_0^p \tilde{\varepsilon}(p', p) \frac{dT^4(p')}{dp'} dp', \quad (3.20)$$

and the upward flux by

$$F^{0\uparrow}(p) = \sigma_B T_G^4 + \sigma_B \int_{p_S}^p \tilde{\varepsilon}(p', p) \frac{dT^4(p')}{dp'} dp', \quad (3.21)$$

where σ_B is the Stefan-Boltzmann constant and T_0 denotes the temperature at the top of the atmosphere. The emissivities ε and $\tilde{\varepsilon}$ correspond to eqs. (11) and (7) respectively, in Sasamori (1968), but in the present application it is assumed that they are functions only of absorbing medium amount between the levels indicated by the indices.

With overcast skies it is assumed that the cloud is a perfect black body. Above the cloud the downward flux is given by eq. (3.20), whereas the upward flux is given by

$$F^{C\uparrow}(p) = \sigma_B T_{CT}^4 + \sigma_B \int_{p_{CT}}^p \tilde{\varepsilon}(p', p) \frac{dT^4(p')}{dp'} dp'. \quad (3.22)$$

Below the cloud the downward flux is given by

$$F^{C\downarrow}(p) = \sigma_B T_{CB}^4 + \sigma_B \int_{p_{CB}}^p \tilde{\varepsilon}(p', p) \frac{dT^4(p')}{dp'} dp', \quad (3.23)$$

and the upward flux by eq. (3.21).

In order to calculate the long-wave cooling rates, the net upward fluxes $F^{\uparrow} - F^{\downarrow}$ in the 200, 600 and 1000 mb levels have to be determined. The net upward flux at 1000 mb is given by

$$F(p_S) = \sigma_B T_G^4 - (1 - CL)\left\{\sigma_B T_0^4 \varepsilon(p_S, 0) + \sigma_B \int_0^{p_S} \tilde{\varepsilon}(p', p) \frac{dT^4(p')}{dp'} dp'\right\} - CL\left\{\sigma_B T_{CB}^4 + \sigma_B \int_{p_{CB}}^{p_S} \tilde{\varepsilon}(p', p_S) \frac{dT^4(p')}{dp'} dp'\right\}. \quad (3.24)$$

Assuming a linear variation of the flux within the cloud, the net flux at the 600 mb level becomes

$$F(p_M) = (1 - CL) F^0(p_M) + \tfrac{1}{2} CL\{F^C(p_{CT}) + F^C(p_{CB})\}, \quad (3.25)$$

where

$$F^0(p_M) = \sigma_B T_G^4 - \sigma_B T_0^4 \varepsilon(p_M, 0) - \sigma_B \int_0^{p_S} \tilde{\varepsilon}(p', p_M) \frac{dT^4(p')}{dp'} dp',$$

$$F^C(p_{CT}) = \sigma_B T_{CT}^4 - \sigma_B T_0^4 \varepsilon(p_{CT}, 0) - \sigma_B \int_0^{p_{CT}} \tilde{\varepsilon}(p', p_{CT}) \frac{dT^4(p')}{dp'} dp',$$

$$F^C(p_{CB}) = \sigma_B T_G^4 - \sigma_B T_{CB}^4 - \sigma_B \int_{p_{CB}}^{p_S} \tilde{\varepsilon}(p', p_{CB}) \frac{dT^4(p')}{dp'} dp'.$$

At the 200 mb level the net flux is given by

$$F(p_T) = (1 - CL)\,\sigma_B\left\{T_G^4 - \int_0^{p_S} \tilde{\varepsilon}(p', p_T)\frac{dT^4(p')}{dp'}dp'\right\} + CL\,\sigma_B\left\{T_{CT}^4 - \sigma_B\int_0^{p_{CT}} \tilde{\varepsilon}(p', p_T)\frac{dT^4(p')}{dp'}dp'\right\}. \quad (3.26)$$

The emissivities used so far have been the total emissivities. They may be expressed in terms of the emissivities of water vapour and carbon dioxide, which are the only gases considered here, as

$$\varepsilon(p', p) = \varepsilon_1(p', p) + L(p', p)\,\varepsilon_2(p', p), \quad (3.27)$$

where the index 1 stands for water vapour and index 2 for carbon dioxide. L is the transmittance function for water vapour near 15 μm where overlapping between absorption bands for water vapour and carbon dioxide occurs. Similarly

$$\tilde{\varepsilon}(p', p) = \tilde{\varepsilon}_1(p', p) + L(p', p)\,\tilde{\varepsilon}_2(p', p). \quad (3.28)$$

Carbon dioxide is assumed to have a constant mixing ratio equal to 300 ppm by volume. The effective path length in centimeters between two levels is obtained (*cf.* Katayama 1972) as

$$U_2(p', p) = 118\frac{|p'^2 - p^2|}{p_S^2}. \quad (3.29)$$

The absorber amount for water vapour U_1 is scaled with pressure in the same way as for short-wave radiation. This means that the effective path length is only a function of the mean surface temperature T_S. For a given value of this temperature, the fluxes are only dependent on the vertical temperature profile $T(p)$. For the long-wave calculations it is assumed that the temperature above the 100 mb level is a prescribed constant equal to T_0. In order to simplify the calculations of the integrals appearing in the flux expressions, the reasonable approximation that T^4 varies linearly with p is used. The layers with constant slope of this temperature function are from 1000 mb to 800 mb, from 800 mb to 400 mb and further to 200 mb, and finally from 200 to 100 mb. The integrals may then be expressed as integrated emissivity functions multiplied by differences of temperature to the 4th power. For example the first integral in the equation for the 1000 mb flux becomes

$$\int_0^{p_S} \tilde{\varepsilon}(p', p_S)\frac{dT^4(p')}{dp'}dp' = ((\tfrac{3}{2}T_1^4 - \tfrac{1}{2}T_3^4) - T_0^4)\int_{p_T}^{p_T} \tilde{\varepsilon}(p', p_S)\,dp' + \tfrac{1}{2}(T_3^4 - T_1^4)\int_{p_T}^{p_3} \tilde{\varepsilon}(p', p_S)\,dp' + (T_G^4 - T_3^4)\int_{p_3}^{p_S} \tilde{\varepsilon}(p', p_S)\,dp'. \quad (3.30)$$

The integrals of the emissivity function can be calculated numerically by dividing the atmosphere into a sufficient number of layers for evaluation of the integrals by the trapezoidal rule. This procedure is, however, a very time-consuming enterprise, if it has to be carried out for every time-step. The assumptions made for the temperature and humidity profiles make it possible to obtain a form in which the fluxes may be expressed as

$$\begin{aligned} F_T &= \sigma_B\{K_{T0}T_0^4 + K_{T1}T_1^4 + K_{T3}T_3^4 + K_{T4}(fT_W^4 + (1-f)T_1^4)\},\\ F_M &= \sigma_B\{K_{M0}T_0^4 + K_{M1}T_1^4 + K_{M3}T_3^4 + K_{M4}(fT_W^4 + (1-f)T_1^4)\},\\ F_G &= \sigma_B\{K_{S0}T_0^4 + K_{S1}T_1^4 + K_{S3}T_3^4 + K_{S4}T_G^4\}, \end{aligned} \quad (3.31)$$

where the Ks are functions only of the mean surface temperature. The long-wave flux calculations are therefore performed by setting up one table for each flux containing values of the Ks for every 5th degree of the mean surface temperature, and then by interpolating in these tables. The number of layers used to evaluate the integrals of the emissivity functions is taken to be 80 between the top and bottom of the atmosphere. The empirical formulae for L_1, $\tilde{\varepsilon}_1$, ε_2 and $\tilde{\varepsilon}_2$ are all obtained from Sasamori (1968), whereas, in order to have a temperature-independent expression, the function ε_1 was derived from eq. (II. 36) in Katayama (1972). In the numerical integrations presented in the following section, the cloud cover is fixed by the values CL = 0.5, p_{CB} = 650 mb and p_{CT} = 550 mb. Examples of the K-coefficients obtained with this cloud cover are given in Table 1.

4. Model results

4.1. *Simulation of the observed climate*

The model described in the foregoing is integrated numerically in time by using a spectral representation of the meridional variation:

$$T(\phi, t) = \sum_{n=0}^{N} T_n(t)\,P_n(\mu),$$

Table 1. *Values of coefficients used in the long-wave calculations according to the expressions (3.31)*

T_S	220	240	260	280	300
K_{T0}	−0.079	−0.079	−0.083	−0.108	−0.137
K_{T1}	0.392	0.437	0.510	0.571	0.617
K_{T3}	0.180	0.196	0.181	0.153	0.115
K_{T4}	0.351	0.290	0.224	0.167	0.125
K_{M0}	−0.053	−0.075	−0.091	−0.103	−0.105
K_{M1}	0.010	0.010	−0.004	−0.014	−0.023
K_{M3}	0.039	0.082	0.116	0.135	0.136
K_{M4}	0.545	0.453	0.355	0.267	0.199
K_{S0}	−0.052	−0.064	−0.069	−0.061	−0.047
K_{S1}	−0.142	−0.117	−0.091	−0.067	−0.048
K_{S3}	−0.295	−0.275	−0.246	−0.208	−0.169
K_{S4}	0.772	0.661	0.537	0.421	0.326

where $P_n(\mu)$ are the Legendre polynomials. The actual truncation is given by $N = 24$ and the transform method (Eliasen *et al.*, 1970) is used with the number of transform latitude circles equal to 38. The time integration is carried out using the leap-frog scheme with a time-step of 1 day, combined with the time filter suggested by Robert (1966). All integrations are commenced from the initial state with the temperature values $T_W = T_L = 288$ K, $T_3 = 275$ K and $T_1 = 241$ K taken from the Standard Atmosphere, and independent of latitude. For T_0, the constant value 205 K is used. From the initial state, the integration in time converges towards a steady state, steady in the sense that the annual cycle is repeated exactly from one year to the next. In order to reach this steady state, the integration must be carried out for a period of about 50 years.

Using for the different parameters the values stated in the foregoing sections, the steady-state solution simulates the observed annual and meridional variations of the zonally averaged temperature quite well. Fig. 1a shows the annual average surface temperature with the solid curve representing the model values and the dashed curve representing observed values given by Warren and Schneider (1979). Similarly the monthly average surface temperature fields for January and July are shown in Figs. 1b and c, respectively. Discrepancies between the model results and the observed data are mainly present in the polar areas, but also the July temperature over the whole northern hemisphere is a few degrees too low, which mainly reflects a failure of about 15 days in the lag between the solar insolation and the temperature. The difference between the land surface temperature and the ocean surface temperature has a large—a somewhat too large—annual variation at high latitudes, which is illustrated by the values for January and July listed in Table 2. This table also includes the model values of the difference, ΔT_S, between the maximum and minimum value of T_S, and for comparison the corresponding observed values. The atmospheric temperature fields at the 800 and 400 mb levels simulated by the model for January and July are shown in Figs. 2a and b, respectively, together with observed zonal mean temperatures taken from Schlesinger and Gates (1979). It is seen that the model reproduces the observed temperatures for January with reasonable accuracy, whereas for July the model temperature at the 800 mb level is somewhat too low to the north of 20° N and at the 400 mb level too high to the south of 20° S.

The radiation quantities are also reproduced

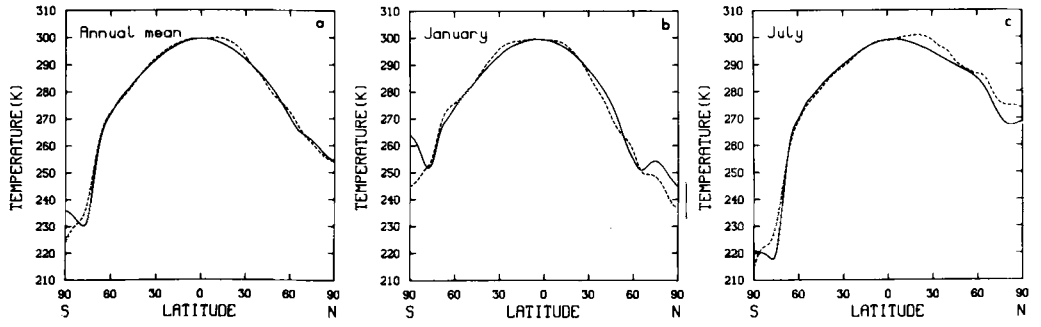

Fig. 1. (a) Simulated annual mean surface temperature (solid curve). Observed data (dashed curve) from Warren and Schneider (1979). (b) Same as (a) but for January. (c) Same as (a) but for July.

Table 2. *Simulated values of $T_L - T_W$ for January and July together with simulated and observed values of seasonal amplitudes of T_S*

	January $T_L - T_W$	July $T_L - T_W$	Model ΔT_S	Observed ΔT_S
90°N	—	—	33.5	37.0
75	−27.2	6.7	22.5	27.6
60	−32.0	11.0	32.2	28.7
45	−13.5	7.7	14.6	21.1
30	−6.6	4.7	7.1	12.7
15	−2.8	2.0	2.8	3.7
0	0.1	−0.5	0.5	1.3
15	2.5	−3.1	3.1	3.3
30	4.3	−5.2	4.8	7.1
45	5.4	−9.5	5.3	4.9
60	6.7	−23.0	7.5	6.9
75	—	—	34.3	26.0
90°S	—	—	45.7	30.3

Table 3. *Values of f and simulated surface and planetary albedos in %*

		January		July	
	f	α_S	α_P	α_S	α_P
90° N	93	75	75	42	50
75	71	75	73	35	47
60	39	59	65	14	32
45	48	28	45	12	29
30	61	13	34	11	27
15	74	10	29	09	26
0	77	09	26	09	26
15	78	09	25	10	29
30	83	09	26	12	33
45	97	08	27	18	40
60	94	13	33	44	57
75	00	85	78	85	83
90° S	00	85	75	85	83

quite well by the model. Table 3 shows the values used for the fraction f of the latitude circle covered by ocean together with the obtained values of the surface and the planetary albedo for January and July. The meridional and seasonal variation of the surface and the planetary albedo are in good agreement with observed values as reproduced for instance in the paper by Robock (1979).

Fig. 3a shows the values obtained for the heat balance in the surface layer of the earth. The dashed curve represents the annual mean value of the net downward radiation flux at the surface, and the solid curve similarly represents the net transport of heat from the earth to the atmosphere. The values are largely in agreement with the generally accepted values as given by Sellers (1965). Between 35° S and 35° N there is a net heating effect of the earth, whereas there is a cooling effect poleward from these latitude circles. The necessary total heat balance at each latitude is produced by horizontal heat transport in the oceans. The seasonal variation of the radiation flux and the small-scale vertical heat transport is illustrated in Figs. 3b and c showing the same two curves as Fig. 3a but for January and July, respectively. The curves for the radiation flux compare quite well with the curves for the corresponding observed radiation flux shown in the paper by Schlesinger and Gates (1979).

The radiation budget for the whole atmosphere–earth system is illustrated in Fig. 4, showing the net downward flux at the top of the model. The solid curve represents the annual mean values, whereas the dashed curve represents the values for January and the dotted curve the values for July. Again the curves for January and July agree

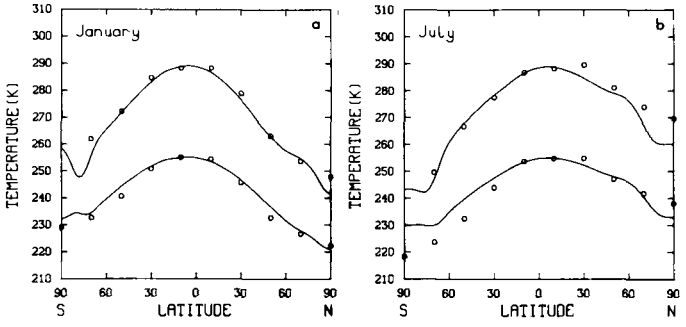

Fig. 2. (a) Simulated temperature fields $T_1(\phi)$ and $T_3(\phi)$ for January (solid curve) and corresponding observed values (indicated by circles) from Schlesinger and Gates (1979). (b) Same as (a) but for July.

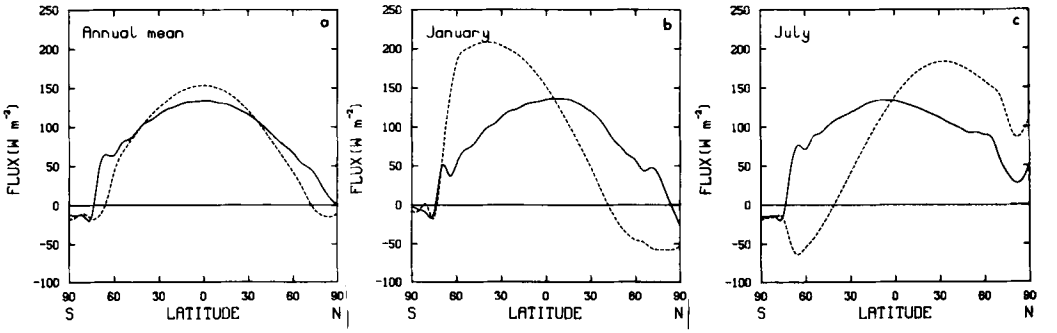

Fig. 3. (a) The annual mean net downward radiation flux at the surface (dashed curve) and the annual mean heat transport from the surface to the atmosphere (solid curve). (b) Same as (a) but for January. (c) Same as (a) but for July.

quite well with the corresponding observed values shown by Schlesinger and Gates (1979). Considering the annual mean values, the total balance required at each latitude is accomplished by horizontal heat transport in the atmosphere and oceans. According to the values obtained from the model, the heat transport carried out by the oceans is about one third of the total transport. The effect of the large-scale atmospheric heat transport in the model is shown in Fig. 5, giving the resulting heating rates in K per day as a function of latitude for January by the solid curve and for July by the dashed curve.

4.2. *Sensitivity experiments*

Several numerical integrations have been carried out in order to test the model's sensitivity to parameter and parameterization changes. A few results are listed in Table 4 giving the changes of the annual mean surface temperature connected with a change of an external parameter of the model.

As seen from Table 4, an increase of the incoming solar radiation by 2% ($\Delta S/S = 0.02$) increases the global mean surface temperature $[T_S]$ by 2.47 K, whereas a decrease of S by 2% decreases $[T_S]$ by 3.28 K. Similar values are obtained from a detailed general circulation model by Wetherald and Manabe (1975). The changes are somewhat smaller in the equatorial area than in the polar regions, where the ice-albedo feedback is effective. Due to the ice-albedo feedback, the temperature changes are essentially larger in the summer than in the winter with no sunshine. The maximum temperature decrease in the case of the lower value of the incoming solar radiation is found to be 15.4 K near the North Pole in August compared with an almost constant decrease of 2.63 K at the equator. The atmospheric temperatures are changed rather similarly

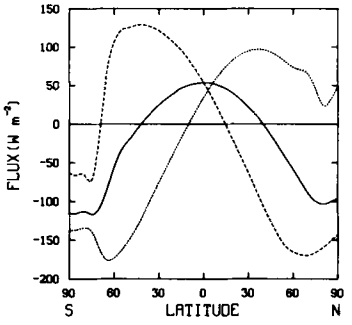

Fig. 4. Net radiation at the top of the model. Annual mean (solid curve), January (dashed curve) and July (dotted curve).

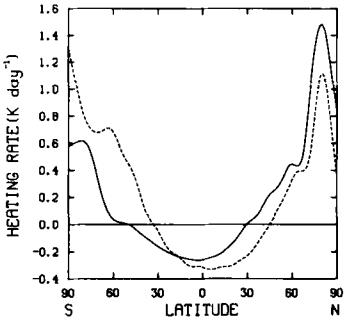

Fig. 5. Total atmospheric heating rates due to large-scale heat transport for January (solid curve) and July (dashed curve).

Table 4. *Changes of annual mean surface temperature resulting from variations of model parameters*

	$\frac{\Delta S}{S} = 0.02$	$\frac{\Delta S}{S} = -0.02$	CO_2 doubling	Change of orbit parameters
90° N	3.98	−5.66	4.72	−3.27
75	3.55	−4.98	4.22	−1.71
60	3.05	−4.26	3.55	−0.80
45	2.57	−3.40	2.74	−0.32
30	2.32	−2.91	2.31	−0.08
15	2.21	−2.68	2.09	0.11
0	2.17	−2.63	2.01	0.19
15	2.21	−2.75	2.08	0.13
30	2.43	−3.06	2.32	−0.03
45	2.58	−3.70	2.71	−0.28
60	3.15	−5.01	3.51	−0.62
75	2.03	−2.49	2.77	−0.61
90° S	2.35	−3.07	3.14	−1.03
$\Delta[T_S]$	2.47	−3.28	2.55	−0.21
$\Delta[T_3]$	2.65	−3.41	2.81	−0.20
$\Delta[T_1]$	2.38	−2.96	2.51	−0.07

to the surface temperature, but with a somewhat smaller variation of the changes with latitude. The changes in T_1 are somewhat smaller than the changes in T_3 and T_S.

The increase of the annual mean surface temperature resulting from a doubling of the CO_2 amount in the model is listed in the third column of Table 4. It is seen that the values are quite close to the values obtained by a 2% increase in the incoming solar radiation. The largest sensitivity is again found in the polar region in late summer. Generally it may be concluded that the sensitivity of the model to changes in the CO_2 content is very well within the limits given by the various results obtained from other simple as well as from much more complex models (*cf.* Schneider, 1975; Manabe and Stouffer, 1979).

The sensitivity of the model to variations in the Earth's orbit, which may be a possible pacemaker of the ice ages (Hays *et al.* 1976) has also been tested. The incident solar flux in the model is computed directly from the three orbit parameters: the eccentricity, the obliquity and the longitude of the perihelion. Steady-state solutions for the model have been obtained for a number of different combinations of possible values of the orbital parameters, and it is found that the most significant decrease of the temperature due to changes of the seasonal insolation occurs for the minimum value of the obliquity, namely 22°, whereas the combined variations within the possible limits of the eccentricity and the longitude of the perihelion seem to be of small importance. The last column in Table 4 shows the changes of the annual mean temperature from the present conditions, in the case of zero eccentricity and obliquity 22°. It is seen that the temperature decreases considerably in the polar regions, especially in the Northern Hemisphere. Considering the seasonal variation of the temperature change, it is found that the temperature decrease is most pronounced during the summer with a maximum value of 12.3 K at the North Pole in August, whereas the temperature in winter is almost unchanged. This result certainly indicates a severe cooling, but the cooling is not extended far enough from the pole to represent a real transition to an ice age.

5. Conclusions

The model presented in this paper is able to give a fair simulation of the observed seasonal and meridional temperature variations at the surface as well as at two tropospheric levels. From this starting-point, it seems worthwhile to improve and extend the model in several directions.

Obviously the effects of water vapour and clouds have been treated very crudely, which might well be the main reason for the deviations from the

observed temperature in the tropical and subtropical areas. In any case, an explicit description of the water vapour content and the variations of clouds would be a desirable feature of the model. Related to this it should also be possible to use a more sophisticated formulation of the small-scale vertical transport of sensible and latent heat.

A clear limitation of the model is the neglect of a direct description of the temperature changes in the atmosphere above the 200 mb level, and certainly it would be of interest to try to explicitly incorporate in the model the effect of the physical processes in the upper atmosphere.

The most serious shortcomings in the present version of the model are presumably connected with the ocean modelling. The occurrence of sea-ice is taken into account only by its influence on the surface albedo. The heat used or released by the change of the amount of sea-ice is not described in the model and this factor is likely to strongly influence the annual temperature cycle in the polar areas.

From the numerical experiments it is found that the response time for the model is about 50 years. An extension of the model to also include the deep-sea is expected to considerably increase the response time and should make it possible to use the model for studies of the long-term externally or internally caused climate fluctuations.

REFERENCES

Berger, A. L. 1978. Long-term variation of daily insolation and quaternary climatic changes. *J. Atmos. Sci. 35*, 2362–2367.

Eliasen, E. 1982. Climate modeling using an equivalent meridional circulation. *Tellus 34*, 228–244.

Eliasen, E., Machenhauer, B. and Rasmussen, E. 1970. On a numerical method for integration of the hydrodynamical equations with a spectral representation of the horizontal fields. Report No. 2, Institute of Theoretical Meteorology, University of Copenhagen, Denmark.

Ghil, M. and Bhattachary, K. 1979. An energy-balance model of glaciation cycles. GARP Publications Series No. 22, 886-916, WMO/ICSU, Geneva, Switzerland.

Hays, J. D., Imbrie, J. and Shackleton, N. J. 1976. Variations in the Earth's orbit: pacemaker of the ice ages. *Science 194*, 1121–1132.

Katayama, A. 1972. A simplified scheme for computing radiative transfer in the troposphere. Technical report No. 6. Department of Meterology, University of California, Los Angeles, USA.

Lacis, A. A. and Hansen, J. E. 1974. A parameterization for the absorption of solar radiation in the Earth's atmosphere. *J. Atmos. Sci. 31*, 118–133.

Langlois, W. E. and Kwok, C. W. 1969. Description of the Mintz-Arakawa numerical general circulation model. Technical report No. 3. Department of Meterology, University of California, Los Angeles, USA.

Manabe, S. and Müller, F. 1961. On the radiative equilibrium and heat balance of the atmosphere. *Mon. Wea. Rev. 89*, 503–552.

Manabe, S. and Stouffer, S. J. 1979. A CO_2-climate sensitivity study with a mathematical model of the global climate. *Nature 282*, 491–493.

Manabe, S. and Strickler, R. F. 1964. Thermal equilibrium of the atmosphere with a convective adjustment. *J. Atmos. Sci. 21*, 361–385.

Robert, A. 1966. The integration of a low order spectral form of the primitive meteorological equations. *J. Meteorol. Soc. Japan 44*, 237–245.

Robock, A. 1979. The performance of a seasonal global climate model. GARP Publications Series No. 22, 766-799, WMO/ICSU, Geneva, Switzerland.

Rodgers, C. D. 1967. The radiative heat budget of the troposphere and lower stratosphere. Rept. No. A2, Planetary Circulations Project, Dept of Meteorology, Massachusetts Institute of Technology, Cambridge, U.S.A., 99 pp.

Sasamori, T. 1968. The radiative cooling calculation for application to general circulation experiments. *J. Appl. Meteorol. 7*, 721–729.

Schlesinger, M. E. and Gates, L. W. 1979. Performance of the Oregon State University two-level atmospheric general circulation model. GARP Publication Series No. 22, 139–206, WMO/ICSU, Geneva, Switzerland.

Schneider, S. H. 1975. On the carbon dioxide-climate confusion. *J. Atmos. Sci. 32*, 2060–2066.

Sellers, W. D. 1965. *Physical climatology*. Chicago and London: The University of Chicago Press.

Sellers, W. D. 1973. A new global climate model. *J. Appl. Meteorol. 12*, 241–254.

Thompson, S. L. 1979. Development of a seasonally-verified planetary albedo parameterization for zonal energy balance climate models. GARP Publication Series No. 22, 1002-1023, WMO/ICSU, Geneva, Switzerland.

Thompson, S. L. and Schneider, S. H. 1979. A seasonal zonal energy balance climate model with an interactive lower layer. *J. Geophys. Res. 84*, 2401–2414.

Warren, S. G. and Schneider, S. H. 1979. Seasonal simulations as a test for uncertainties in the parameterizations of a Budyko-Sellers zonal climate model. *J. Atmos. Sci. 36*, 1377–1391.

Wetherald, R. T. and Manabe, S. 1975. The effect of changing the solar constant on the climate of a general circulation model. *J. Atmos. Sci. 32*, 2044–2059.